The Spherical Probe Electric Field and Wave Experiment for the Cluster Mission

G. Gustafsson, R. Boström, B. Holback, G. Holmgren, K. Stasiewicz
Swedish Institute of Space Physics, Uppsala, Sweden

T. Aggson, R. Pfaff
NASA, GSFC, Greenbelt, MD 20771, USA

L.P. Block, C.-G. Fälthammar, P.-A. Lindqvist, G. Marklund
The Royal Institute of Technology, Stockholm, Sweden

C. Cattell, F. Mozer, I. Roth, M. Temerin, J. Wygant
University of California, Berkeley, CA 94720, USA

P. Décréau
LPCE/CNRS, Orléans,France

A. Egeland, J. Holtet, E. Thrane
University of Oslo, Oslo, Norway

R. Grard, J.-P. Lebreton, A. Pedersen, R. Schmidt
SSD/ESTEC, Noordwijk, The Netherlands

D. Gurnett
University of Iowa, Iowa 52242, USA

C. Harvey, R. Manning
Observatoire de Paris-Meudon, France

P. Kellogg
University of Minnesota, Minneapolis, USA

P. Kintner
Cornell University, Ithaca, NY 14853, USA

S. Klimov
Space Research Institute, Moscow, Russia

N. Maynard, H. Singer, M. Smiddy
Phillips Laboratory, Geophysics Directorate, MA 01732, USA

K. Mursula, P. Tanskanen
University of Oulu, Oulu, Finland

A. Roux
CRPE/CNET,Issy-les-Moulineaux, France

L.J.C. Woolliscroft
University of Sheffield, U.K.

The electric field and wave experiment (EFW) on Cluster is designed to measure the electric field and density fluctuations with sampling rates, on some occasions, up to 36 000 samples/s in two channels. Langmuir sweeps can also be made to determine the electron density and temperature. Among the more interesting objectives of the experiment is to study nonlinear processes that result in acceleration of plasma. Large-scale phenomena where all four spacecraft are needed will also be studied.

Keywords: Electric field, Electron density, Waves, Boundary regions, Cluster mission, Langmuir probe.

Abstract

1. Scientific background

1.1 Introduction

The Cluster spacecraft will pass through numerous plasma regimes separated by a variety of boundaries and discontinuities. From the view point of an electric field and plasma fluctuation experiment, this means that a large variety of wave/wave, wave/particle and nonlinear plasma interactions as well as time and space variations of macroscopic and quasi-static electric fields will be found along the trajectory of the spacecraft. These phenomena will occur over widely differing temporal, spatial, and amplitude ranges. To provide an adequate understanding of the phenomena, an electric field and plasma fluctuation experiment must be able to measure, in two dimensions, over frequencies ranging from DC to 10 kHz with a time resolution of 100 ms. This will cover wave frequencies up to the frequency of lower hybrid modes, and the time resolution will resolve time-domain structures. Amplitudes of a few microvolts/m to 700 mV/m have to be covered and plasma density fluctuations from about 1 to 50% relative variation. It should be able to measure phase velocities of electrostatic structures over time scales of milliseconds by interferometric timing between opposing boom pairs. In order to measure the polarisation of electrostatic waves and resolve the **k** vectors of waves propagating perpendicularly and parallel to the magnetic field with frequencies greater than the spin rate of the spacecraft, it must have two pairs of electric-field sensors, which can be sampled to produce an instantaneous two-dimensional electric-field vector. The operational mode, with all four probes measuring density fluctuations, will permit two-dimensional plasma-wave interferometer measurements that will make it possible to determine wavelength, phase velocities and time of flight of plasma phenomena. Finally, it must have an internal burst memory in order to record high-time-resolution data at rates higher than the telemetry stream. This burst memory should be large enough to permit sampling over the spatial distances associated with the bow shock, auroral structures, the plasma-sheet boundary, and the magnetopause.

1.2 Electric fields at small scales

Some of the most interesting magnetospheric physics is associated with nonlinear processes that result in the acceleration of plasma. S3-3, Viking and ISEE electric-field measurements have shown that particle acceleration is associated with large-amplitude, short-duration electric-field signatures (see Figs. 1 and 2). Small spatial- and temporal-scale structures are important because they provide the necessary dissipation in the various magnetospheric boundary regions. They are equally important from the point of view of basic plasma physics: they represent the nonlinear state of the plasma under various conditions.

Since such structures are inherently nonlinear, it is desirable to study them in the time domain. The use of time-domain information nicely complements the spectral information that is important in the study of linearly propagating waves. The investigation of nonlinear structures in the time domain provides the best opportunity to make new discoveries by exploiting the capabilities made possible by recent advances in technology.

ISEE observations in the bow shock reveal intense electric field spikes with ampli-

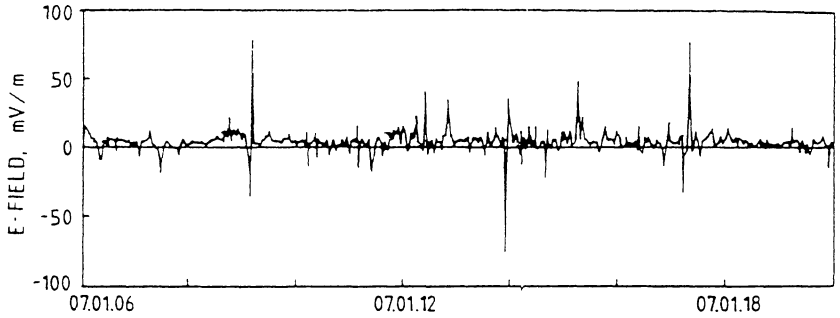

Figure 1. Measurements on ISEE-1 at 32 samples/s of spiky electric fields of about 100 mV/m and a duration of 0.05 s during a bow shock crossing. This is a single-axis measurement, so the direction relative to the magnetic field of the spikes is not known. Similarly no information of the phase velocity is available from this measurement. On Cluster, the phase velocity could be determined if the signals from the four probes were available at sampling rates of up to 9000 samples/s.

tudes of 100 mV/m and a duration of 0.05 s (Fig. 1). The spikes are often bipolar.

Almost none of the properties of these waves can be determined by the ISEE experiment but could be determined by the Cluster quasi-static experiment. The phase velocity, scale size, polarisation relative to the ambient magnetic field, three-dimensional structure, coherence length, relation to comparable temporal-scale density and magnetic-field fluctuations can be determined with the Cluster electric field instrument in four satellites. These quantities are needed to evaluate the role of the spikes in providing anomalous resistivity, thermalising ion and electron distributions, and in the production of high-energy electron beams commonly seen at the bow shock.

High-time-resolution data must be obtained using the internal burst memory in various different sampling schemes based on the region of space being sampled. Whenever higher-time resolution data have become available, new phenomena have been discovered, e.g. recent rocket observations of Langmuir solitons [1]. We anticipate the discovery of many interesting important new structures in the high-frequency time-domain data to be obtained by the Cluster satellites.

1.3 Electric fields at intermediate scales

Many of the central scientific goals of the Cluster mission relate to electric fields at intermediate scales (100's of km to a few R_E). These include MHD turbulence in the solar wind, magnetosheath and cusp, instabilities driven by velocity shears, waves associated with quasi-parallel shocks, transfer events, impulsive penetration of plasma into the magnetosphere, and slow-mode shocks in the near tail in association with reconnection. Electric-field data will provide information which is vital for determining wave modes, wave vectors, phase velocities and energy flow. The spatial and temporal variation in the auroral-zone electric field is another interesting topic addressed by measurements on these spatial scales.

The average behaviour of the auroral-zone electric field and related electrodynamical parameters for various geophysical conditions is relatively well documented. This is not the case, however, for the instantaneous auroral electrodynamics, on which very few studies have been conducted [2,3]. A new technique for obtaining global realistic and self-consistent distributions of auroral electrodynamical parameters has been recently developed [3]. Simultaneous observations on the different spacecraft involved are used both for calibration of the model input data (field-aligned currents and conductivities) and for tests of the results (equipotential pattern). For studies of this kind, the Cluster mission with simultaneous four-point measurements will be ideally suited.

The electric field is an important parameter in the measurement of MHD turbulence. MHD turbulence is expected in all the important regions to be investigated by Cluster. The electric field, together with the magnetic field, determines the Poynting flux and the propagation direction of the waves and plasma flows in these regions. The scale size and the magnitude of the electric fields involved have a wide range of values in

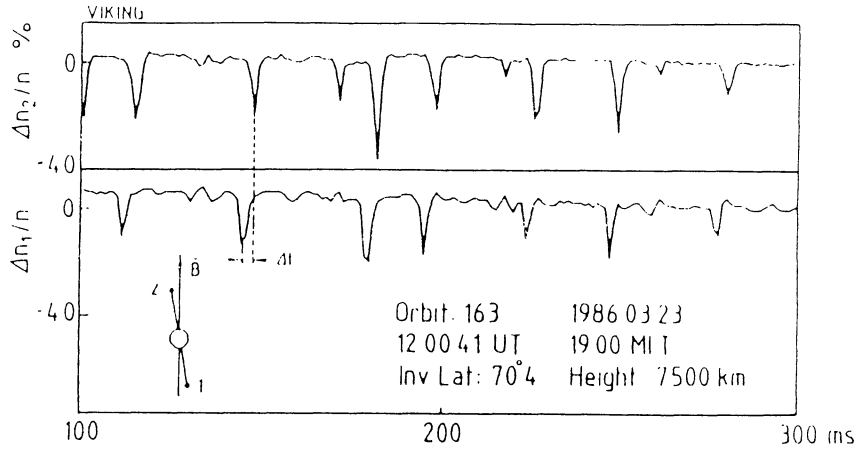

Figure 2. Weak double layers observed on Viking. These measurements from Viking show high-time-resolution density-fluctuation data in two channels. The instrument was also able to measure one electric field vector and one density fluctuation parameter simultaneously. From these data rather detailed characteristics of weak double layers could be obtained such as propagation velocity and direction, scale length, net electric field etc. [14]. On Cluster similar phenomena could be studied in other regions of space and scale lengths in two directions with a time resolution of a millisecond or better.

these various regions. In the solar wind, scale sizes are several hundred kilometres to many thousands of kilometres and electric-field magnitudes are of the order of 1 mV/m. On auroral field lines, the electric field is typically much larger. Magnitudes of over 100 mV/m are common on scale sizes from less than a kilometre to tens of kilometres [4,5,6]. The quasi-parallel shock structure provides a strong challenge to space physicists attempting to understand the role of different wave modes and scale sizes in the decelaration and thermalisation of upstream plasma. The four Cluster spacecraft can determine the phase velocity and Poynting flux waves and "shocklets" upstream and downstream of the shock. In the absence of such measurements it would be difficult to distinguish between waves standing in the shock frame, waves created in the upstream region and convected and amplified across the shock transition region, and waves created in the transition region.

1.4 Electric fields at large scales

At the longest scale lengths of interest for the Cluster study are the electric fields associated with processes such as steady-state reconnection at the magnetopause, convection in the "quiet" magnetotail, and the formation of a near-earth neutral line.

Steady-state convection in the magnetotail has been examined by analytic and numerical methods as well as simulations [7,8]. It will now be possible for the first time to test the resulting models with the aid of the Cluster electric-field data. ISEE-1 electric-field data have suggested that the electric fields associated with the hypothesised near-earth neutral line are confined to approximately 10-15 R_E in the dawn-dusk direction [9,10]. Comparisons of observed electric fields in the tail (20-40 mV/m during candidate neutral-line events) with cross-polar-cap potentials imply that the field is primarily inductive [10,11]. The Cluster satellite electric- and magnetic-field data will permit direct determination of associated electric fields, the relative importance of inductive and potential fields, as well as the relationship of the neutral line propagation speed to the electric field and where reconnection is initiated in the plasma sheet. The four satellites will also make it possible to determine the extent of substorm electric fields which may not be directly related to the neutral line [12], in particular they may show how these fields are related to substorm injection. Preliminary results on the propagation of these electric fields obtained by comparing the ISEE-1 and Geos data have been published [11]. Comparisons of the $\mathbf{E} \times \mathbf{B}$ velocity to plasma-sheet-boundary motions [13] have shown that the two agree during plasma-sheet contraction, but not during expansion. Cluster electric-field data can provide additional, more detailed information that will assist us to understand plasma-sheet motion, in particular, variations in the dawn-dusk and earthward-tailward directions.

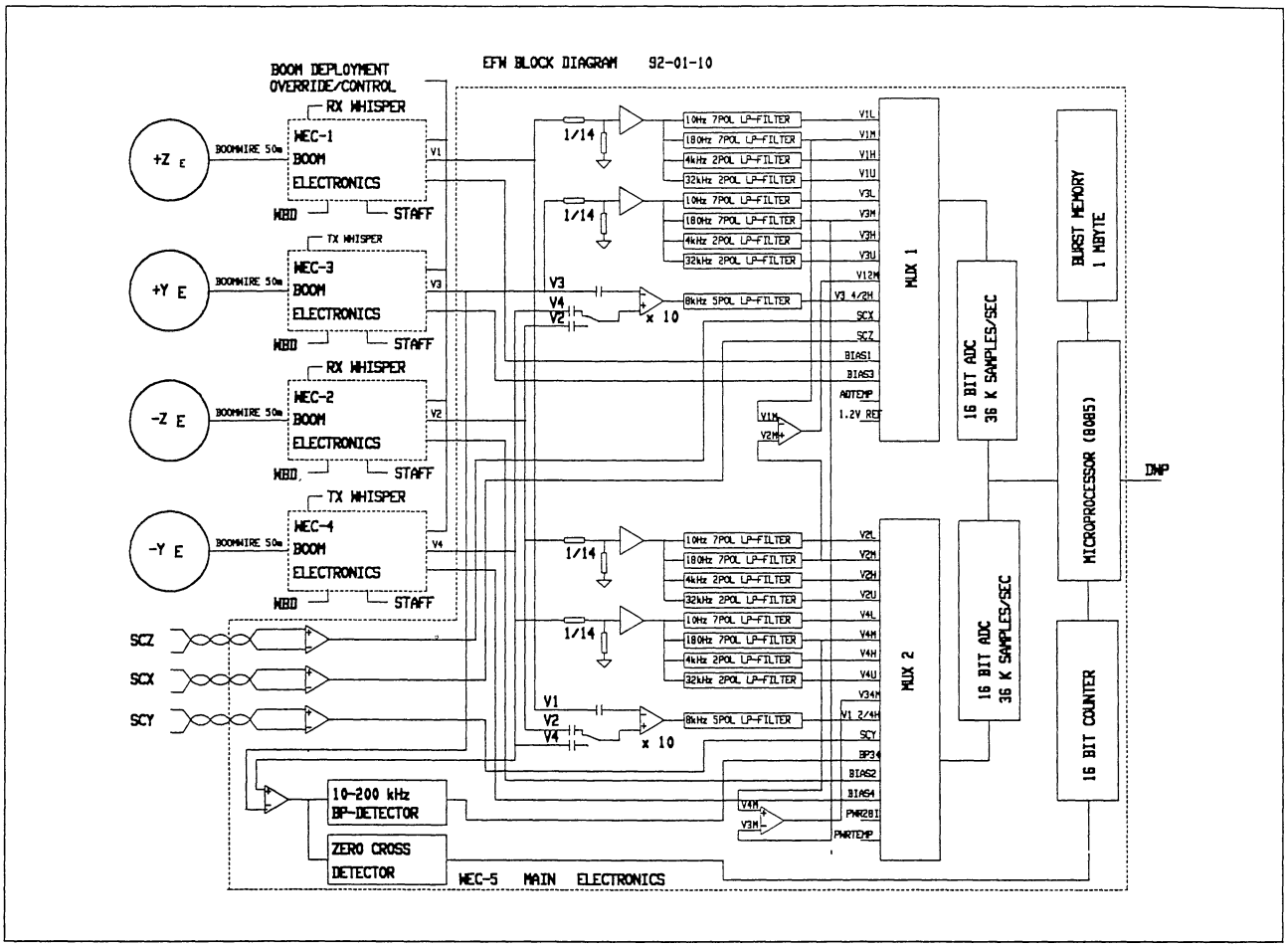

Figure 3a. Block diagram of EFW.

2. Instrument description

2.1 General

To meet the scientific objectives, the electric field instrument will be capable of measuring, in various modes:

- Instantaneous spin-plane components of the electric-field vector, over a dynamic range of 0.1 to 700 mV/m, and with variable time resolution down to 0.1 ms.
- The low-energy plasma density, over a dynamic range of at least 1 to 100 cm^{-3}.
- Electric fields and density fluctuations in weak double layers of small amplitude, over dynamic ranges of 0.1 to 50 mV/m for the fields and 1 to 50% for the relative density fluctuations, and with a time resolution of 0.1 ms on some occasions.
- Electric fields and density fluctuations in electrostatic shocks or double layers of large amplitude, over dynamic ranges of 0.1 to 700 mV/m for the fields and 1 to 50% for the relative density fluctuations, and with a time resolution of 0.1 ms on some occasions.
- Waves, ranging from electrostatic ion cyclotron emissions having amplitudes as large as 60 mV/m at frequencies as low as 50 mHz, to lower hybrid emissions at several hundred hertz and with amplitudes as small as a few microvolts per metre.
- Time delays between signals from up to four different antenna elements on the same spacecraft, with a time resolution of 30 μs on some occasions.
- The spacecraft potential.

The detector of the instrument consists of four orthogonal spherical sensors deployed from 50 m cables in the spin plane of the spacecraft, four deployment units, and a separate main electronics unit as shown in the block diagram in Figures 3a and b. The

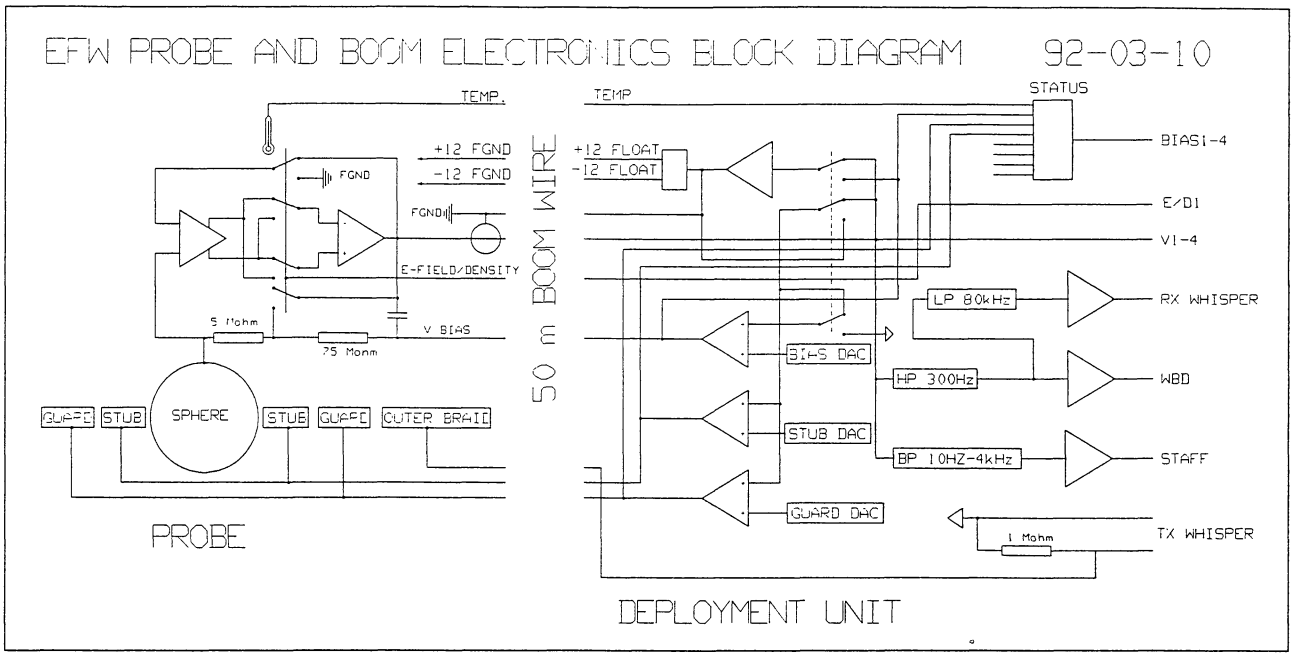

Figure 3b. Block diagram of EFW (continued).

instrument has several important features. The potential drop between two opposing spherical sensors can be measured to provide an electric-field measurement. The instrument can also be operated as a Langmuir probe and biased to provide the Langmuir current/voltage curve and, thus, to measure the electron temperature and density. The potentials of the spherical sensor and nearby conductors are controlled by the microprocessor in order to minimise errors associated with photoelectron fluxes to and from the spheres. The output signals from the spherical sensor preamplifiers are provided to the wave instruments for analysis of high frequency wave phenomena. The instrument has a 1-Mbyte burst memory and two fast A/D conversion circuits for recording electric-field wave forms for time resolutions up to 36 000 samples/s. Data gathered in the burst memory will be played back through the telemetry stream allocated to the electric-field experiment by pre-empting a portion of the real time data gathered by the instrument. On-board calculations of least-quare fits to the electric-field data over one spacecraft spin period (4 s) will provide a baseline of high-quality two-dimensional electric-field components that are present in the telemetry stream, except for periods when three or four sensors are in current mode. Incoming data are continuously monitored by means of algorithms in the software to determine whether conditions are appropriate for triggering a burst-collection playback. The spacecraft potential is calculated and transmitted via DWP to other instruments on board.

2.2 Analog electronics

Each sphere houses a preamplifier which measures the potential difference between the sphere surface and the spacecraft analog ground. Since the plasma has high source impedance (10^7-10^{10} Ω) and a capacitance of 5 pF due to the 8 cm diameter sphere, the preamplifier must have a low leakage current (< 10 pA) and low input capacitance (8 pF) to avoid the attenuation of input signals. Since the potential of a biased sphere can differ from that of the spacecraft by up to 30 V in the absence of an electric field, and fields as large as 500 mV/m have been observed, the dynamic range of the preamplifier and associated sensor electronics is ± 70 V from DC to 200 Hz (see Fig. 4). The small signal response exists to 600 kHz for use by the AC electric-field instrument.

The 50-metre boom cable between the deployment unit and the sphere sensors contains eight wires and one coaxial cable. These wires carry the power to the preamplifier in the sphere, the biasing voltages on the stub and guard surfaces near the spheres,

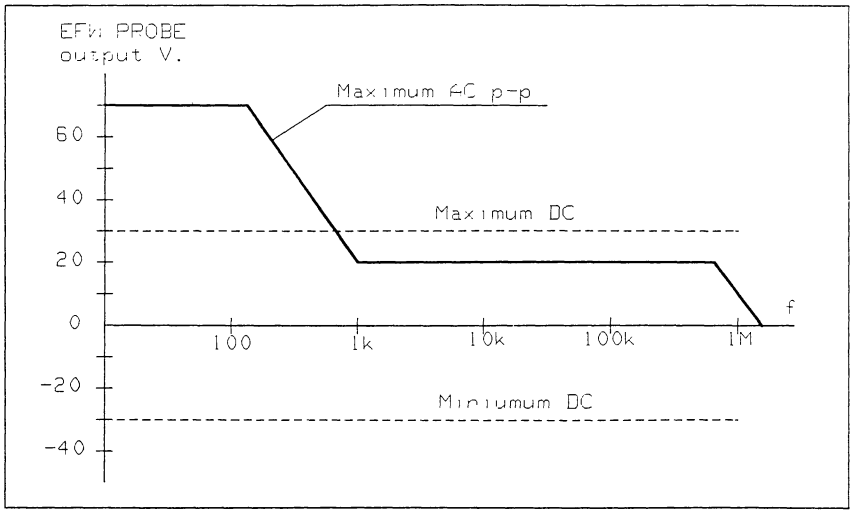

Figure 4. Probe amplifier output vs frequency is shown. The background DC level is expected to vary between ±30 V and superimposed on that is the maximum AC variation shown. As an example of an extreme case; if we assume a 30 V DC level, then a superimposed ±70 V AC signal at 100 Hz and at the same time a ±20 V AC signal at 10 kHz is still within the operational range of the instrument.

and the biasing voltage to the bias resistor. The wires and coaxial cable are surrounded by a kevlar braid which provides mechanical support against the centrifugal stresses on the cable. The outer surface of the cable is a conductor which is tied to the spacecraft EFW main ground chassis.

In order to limit and control the flux of photo-electrons from the booms to the spherical sensors and to minimise error, sources in the potentials of stub and guard surfaces are forced to follow the potential of the sphere with an adjustable DC offset. The DC offset is determined by 8-bit microprocessor-controlled digital-to-analog converters located in the digital section of the main electronics box. The stub voltage follows the sphere voltage with an offset which can range between −1.26 and +1.26 V in 256 steps. The guard voltage follows the sphere potential with an offset between −39 and +39 V in 256 steps.

The sphere potential is determined by the balance of plasma thermal currents, photoemission current, and a bias current to the sphere whose magnitude is controlled by on-board electronics to minimise the sheath impedance. This is accomplished by controlling the potential drop across the bias resistor of Figure 3 with bias-control circuitry. One end of the bias resistor is tied to the sphere surface. The other end of the resistor is driven by the bias-control circuitry which operates in one of the two modes as determined by the state of a bias relay. If the instrument is measuring electric fields, the relay is set so that the bias-control circuit follows the output of the sphere with a DC offset determined by the digital-to-analog converter (DAC). The potential drop across the resistor is the DAC-determined value and the injected current is this value divided by the value of the resistance. This current can vary from −0.5 to +0.5 μA in 256 steps. These values are large enough to balance the maximum possible photoelectron flux from the spheres.

The spherical sensors can also be operated as current-collecting Langmuir probes to provide information on the plasma density and electron temperature. In this mode, relays in each of the four deployment units are flipped so that the microprocessor-controlled bias circuits are referenced to the satellite rather than to the output of the sphere preamplifier.

The output of each sphere preamplifier is filtered by anti-aliasing filters. A simple frequency counter is included to monitor the plasma frequency. The lowest-frequency filter data will be utilised for direct transmission of data. The intermediate frequency signal will be stored on the on-board tape recorder. The highest-frequency data will be recorded in the internal burst memory and played out at slower telemetry rates or

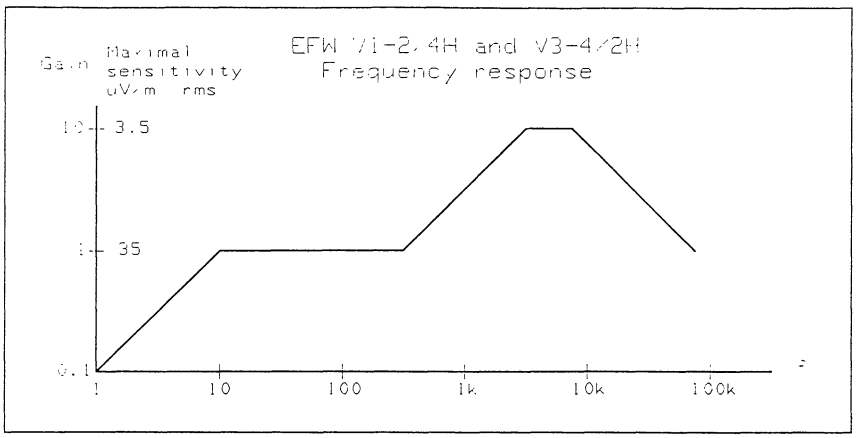

Figure 5a. A diagram of the sensitivity versus frequency. The sensitivity for the 8 kHz filter is shown with the factor of 10 in amplification.

in a special telemetry mode at high rate. For details, see Section 4.

2.3 Digital electronics

The digital electronics contain two very fast, 16-bit, analog-to-digital systems, a set of digital-to-analog converters for biasing, a single 8-bit radiation-hard microprocessor, and a 1-Mbyte burst memory. Extensive software functions increase the instrument's capabilities and data coverage.

The strategy for measuring the sphere voltages over a range of plus or minus 700 mV/m to a relative accuracy of 3 μV/m can be achieved in a number of ways. With a 16-bit converter, the single-ended measurements of sphere voltage (V1 through V4) will be measurable from 700 mV/m to 30 μV/m. Differential measurements between V1-V2/4H and V3-V4/2H will have a gain factor of ten and thus be measurable to about 3 μV/m taking the system noise into account (the one-bit resolution is 0.15 μV/m), but will only have a range to 10 mV/m. The variation of the sensitivity with frequency of the instrument is shown in Figure 5a and the one-bit resolution in Figure 5b.

2.4 Boom-deployment mechanism

Each DC electric fields deployment unit is a small, self-contained package containing a motor-driven mechanism that deploys a multiconductor cable and tip-mounted spherical sensor in the spin plane of each Cluster satellite. In orbit, each opposing pair of cables will be symmetrically deployed to a tip-to-tip distance of approximately 100 m, except for about a week at the beginning of the mission when 70 m will be used for one boom pair (the z booms) and 100 m for the other pair. The assembly consists of two major components: a deployment mechanism, and the cable with sensor. The mechanism design has evolved from a series of successful satellite experiments including S3-2 and S3-3, ISEE, Viking, and CRRES. The deployment unit contains a rotating assembly, a brush DC gear motor, an over-tension and end-of-cable indicator, an analog cable-length indicator, a pyrotechnic-released spherical sensor housing, and a cable oscillation Coulomb damper, through which the cable exits from the mechanism. The possibility that the satellite control deploys the booms is also built into the system.

The Engineering Model is shown in Figure 6.

3. EFW operational modes

The EFW instrument has a large number of possible sampling modes. The main parameters to be selected in each case are: probe bias, probe mode, filter frequency, telemetry rate and internal memory use. Several of the parameters are interrelated, which limits the possible number of combinations, and the telemetry rate is also dependent

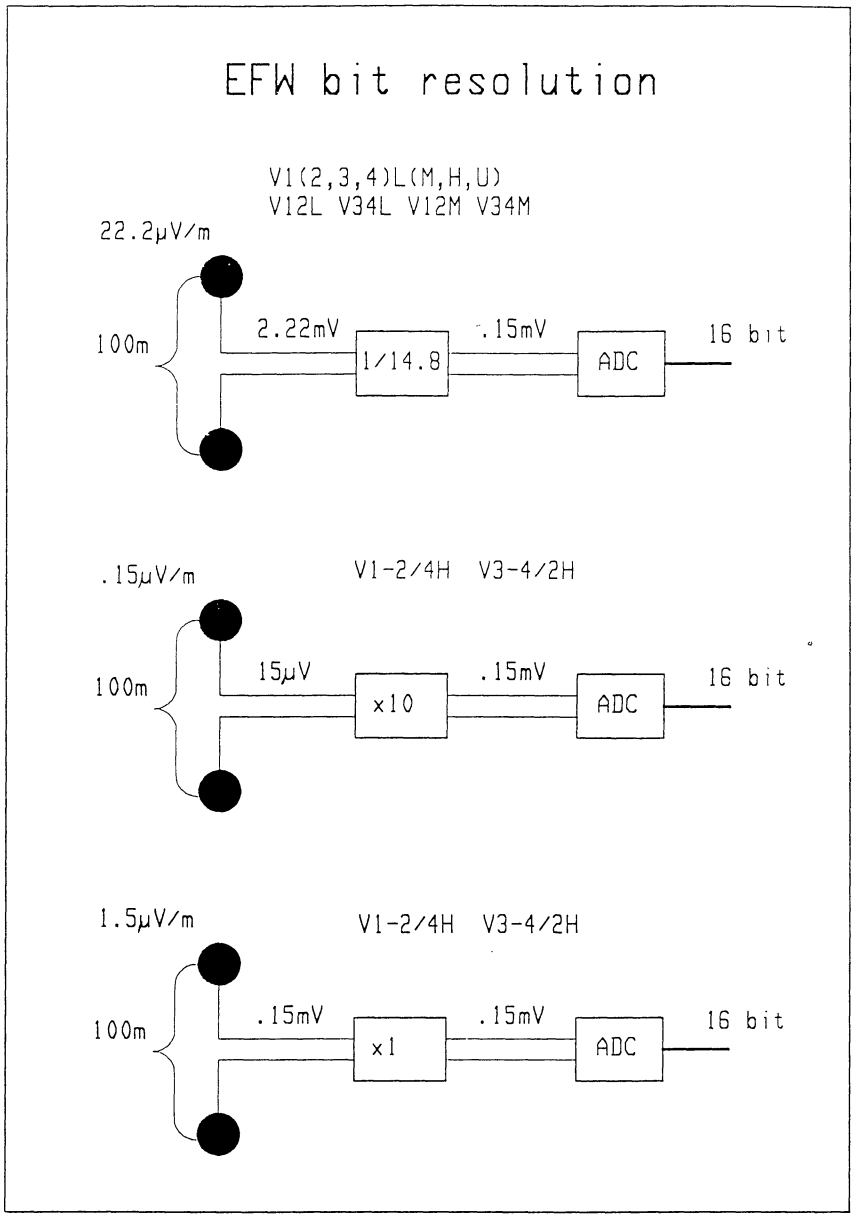

Figure 5b. The noncalibrated one-bit resolution of the instrument from probe through ADC.

on other instruments in the wave consortium. The combinations of probes and telemetry is shown in a schematic way in Figure 7.

The four probes can all be operated individually in current mode (to measure density/temperature), or voltage mode (to measure electric field) see Figure 7. In some combinations, voltages are measured from probe to satellite and in some cases differentially between two probes. The three components from the search coil instrument are also available in EFW with a bandwidth of 4 kHz.

A diagnostic sweep, of 1-2 seconds duration, is performed approximately every 30 minutes. A bit in the EFW telemetry will indicate the occurrence of the sweep.

Each probe signal is transferred through an anti-aliasing filter and sampled by one of the two A/D converters. Low-pass filters at 10 Hz, 180 Hz, 4 kHz, or about 32 kHz, or a bandpass filter for 50 Hz to 8 kHz are available. The telemetry limits the direct transmission to 10 Hz (25 samples/s) and the transmission to the tape recorder to

Figure 6. EFW Engineering Model: the model consists of two complete boom units with electronics (units 1 and 2) and two units (3, 5; 4, 6) with electronics only. the flight models will have four boom units. The various parts are:

1 and 2: Boom mechanism with motors, wire, sphere and electronics. Mechanical parts are made at University of Oulu and SSL, Berkeley; integration and tests are peformed at SSL, Berkeley.

3 and 4: Electronics boards are made at KTH, Stockholm.

5 and 6: Buffer boards are made at IRF-Uppsala.

7: DC/DC converter is made at SSL, Berkeley.

8: Main electronics boards are made at SSD, ESTEC.

180 Hz (450 samples/s). Frequencies above that may be recorded with the internal burst memory. There is also a simple frequency counter and an rms detector for 10-200 kHz available to detect the plasma frequency.

The data transfer from EFW to telemetry goes via DWP and can be made at four different rates: 1440, 15 040, 22 240, or 29 440 bit/s.

The main probe combinations for each of the EFW data modes are shown in Figure 7. Each square of the figure shows one combination of probes for a particular data transmission rate, shown as one row. As an example, mode EFW1a corresponds to two perpendicular vector measurements of the electric field, giving a total data rate of 1440 bit/s. After experience has been gained with the instrument in orbit, the number of combinations may be reduced. There is also a possibility, not shown in Figure 7, to measure two parallel electric-field vectors separated in space in mode EFW2a.

EFW carries out on-board estimates of the spacecraft potential that are sent to DWP for distribution to other instruments. For this calculation, at least two probes operated in the voltage mode are required, which is not the case when three or four probes are operated in current mode. EFW also has the capability to make on-board preliminary estimates of the DC electric field by means of spin-fit calculations.

The EFW internal memory storage will be used to register signals from the filters with frequencies of 0-4 kHz, 50 Hz to 8 kHz and 0-32 kHz, as data from these frequencies cannot be transmitted in real time owing to telemetry limitations. The 4, 8, and 32 kHz signals are sampled at 9, 18 and 36 ksamples/s, respectively, and are stored in the internal memory, which can be triggered by ground commands or by an internal algorithm based on EFW data or on flux-gate-magnetometer data via DWP.

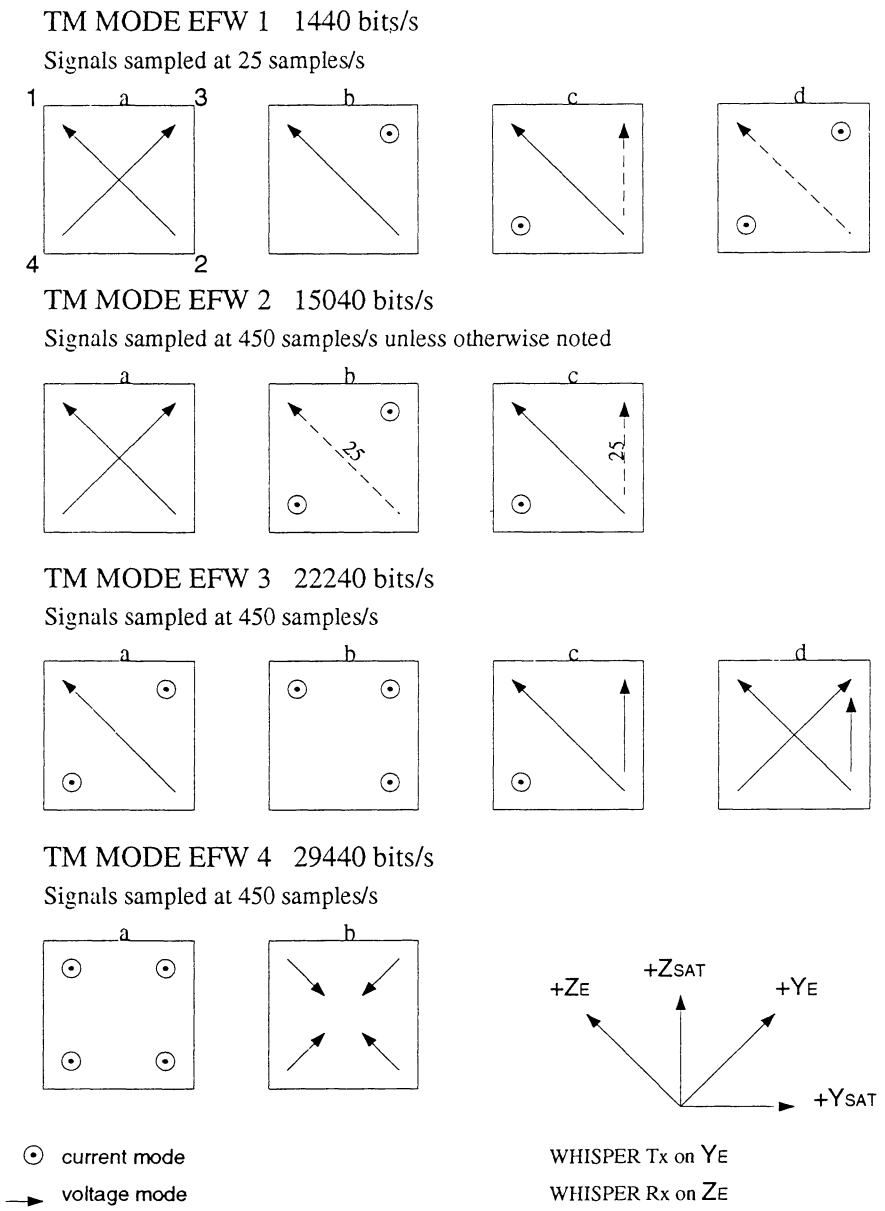

Figure 7. The software and hardware has been made to accommodate the probe combinations shown in each of the boxes in the figure. The broken lines indicate that these modes imply some compromise regarding the content of the telemetry format to get sufficient space.

4. On-board data handling and telemetry

4.1 Data handling

The Cluster EFW instrument communicates with DWP by a single 38.4 kbit/s serial link. EFW accepts commands, telemetry codes and flux-gate-magnetometer data (8 vectors/s) from the DWP unit, and transmits telemetry data to DWP.

The EFW software co-ordinates real-time sampling along with burst (high sampling rate) data collections using an 80-element sampling buffer. The total A/D rate is 36 000 sample-pairs per second, which fills 450 buffers per second. EFW software must allocate samples from this total collection rate to real-time samples, burst samples, boom monitoring, sweep-collection points etc. The user controls how much of the samples may be used for real-time and non-burst data and how much can be used by bursts.

There are four 'sample' modes available: Normal, Split, Hx only and Null. In the Normal mode, all real-time and monitoring samples are allowed while burst operations are limited to 9000 sample-quadruples per second.

The Split mode allows the user to push the burst data sampling to 18 000 sample pairs. In this mode, the real-time samples are taken 1/18 000 of a second apart instead of 1/36 000.

The Null mode turns off real-time and monitoring and allows the burst to take all 36 000 sample-pairs; the telemetry is undefined in this case.

The Hx only mode is a variation of the Null mode. The burst data can take all 80 elements of the sampling buffer, but V12 and V34 data are available to telemetry every 40 sample-quadruplets.

4.2 Telemetry description

The EFW instrument sends telemetry data in blocks to DWP. Each of the four data rates has its own blocking format, as shown in Figure 8. Basically, data is blocked up for transmission in different ways, depending on the mode. In mode EFW1(1440 bit/s), data is transferred in a single block once per second. For modes EFW2-4, 10 blocks per second are sent to DWP, making up one format.

4.3.1 Fast digital monitor

The purpose of the Fast Digital Monitor (FDM) is to indicate relatively fast mode transitions and status of the telemetry stages. For example, playbacks of recorded data are indicated by a playback bit in the FDM. See Figure 8 and description below for the bit structure.

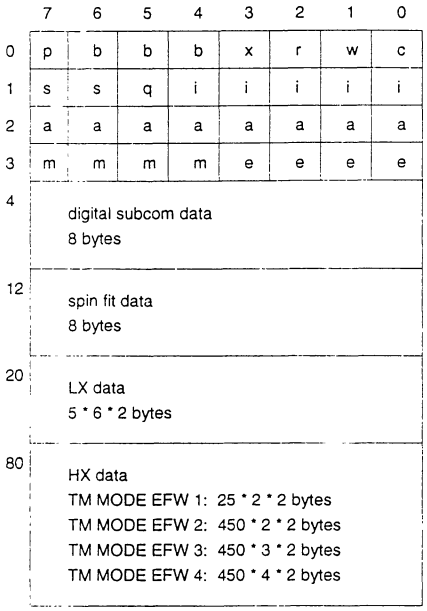

Figure 8. Telemetry format.

p	playback indicator 0 – off 1 – playback in progress
bbb	burst internal state 000 – off 001 – compiling list 010 – turning on 011 – searching 100 – collecting 101 – closing the file 110 – playback wait 111 – playing back
x	main/burst playback 0 – burst playback 1 – main playback
r	whisper pulses present if set
w	sweep in progress if set
c	command counter mismatch if set
ss	sampling mode 00 – NORMAL 01 – SPLIT 10 – HXONLY 11 – NULL
q	interferometric mode if set
iiiii	digital subcom index

aaaaaaaa	sun angle
eeee	voltage/current mode for each probe (,,4,3,2,1†) 0 – voltage mode 1 – current mode
mmmm	motor on/off status for each boom unit (,,4,3,2,1†) 0 – off 1 – on

4.3.2 Spin-fit data

The EFW instrument calculates the E-field vector by taking 32 points at equal angles and fitting a sine wave least-squares fit to the data. The resulting values are represented as 3-byte floating-point values.

4.3.3 Digital subcom data

The digital subcom data consist of a 256-byte table which is intended to telemeter very slow instrument status, verify commanding etc. For each format, 8 bytes of digital subcom data are sent, which means that it takes 32 formats (32 seconds) to construct the table.

4.3.4 LX data (Low-rate data)

In the normal case, this area is used for the V1L, V2L, V3L and V4L quantities sampled at 5 samples/s. Other quantities and burst playback data can also be routed through this section. All values are little-endian 16-bit 2's complement numbers.

4.3.5 HX data (High-rate data)

In tm mode EFW 1, this section contains 25 samples each of V12L and V34L by default. The content can be changed to other quantities and burst playback data by command. All values are little endian 16-bit 2's complement numbers.

5. Instrument summary

The main characteristics of the instrument are: high sampling rate capability, two-dimensional electric field measurements and two-dimensional plasma interferometer measurements with four Langmuir probes. Three main parameters will be measured: (i) The quasi-static electric field; (ii) The wave electric fields; (iii) The plasma density and the relative density fluctuations. The main parameters of the instrument are listed in Tables 1 to 3.

Table 1

Measured quantity	Frequency range	Dynamic range
DC Electric Field (2 components)	0 – 10 Hz	700 mV/m – 0.1 mV/m
	0 – 180 Hz	700 mV/m – 0.1 mV/m
	0 – 4000 Hz	700 mV/m – 0.1 mV/m
	0 – 32000 Hz	700 mV/m – 0.1 mV/m
AC Electric Field (2 components)	10 – 8000 Hz	10 mV/m – ≈3 μV/m
Plasma density fluctuations	0 – 10 Hz	1 – 100 cm^{-1}
	0 – 180 Hz	1 – 100 cm^{-1}
	0 – 4000 Hz	1 – 100 cm^{-1}
Frequency counter	10 – 200 kHz	
Density and temperature (Langmuir sweeps)		1 – 100 cm^{-1} eV range

Table 2

Data rates

Nominal telemetry rate	1 440 bit/s
Tape loading mode data rates	15 040 bit/s 22 240 bit/s 29 440 bit/s
Burst memory loading mode data rate	≲1132 kbit/s

Table 3

Physical Data

Item	Mass (kg)	Power (W)
Main electronics box	1.80	3.7
Wire booms (4 units)	13.60	

6. Distribution of responsibilities among institutes

The Swedish Institute of Space Physics in Uppsala is responsible for the overall leadership of the project, with G. Gustafsson as PI, L. Åhlén as technical manager and G. Holmgren/ A. Lundgren managing data handling and software, respectively. The laboratories in Berkeley, Noordwijk, Oslo, Oulu, Stockholm and Uppsala are responsible for the design, production, test and integration of various parts of hardware. The main responsibility for flight software is with Berkeley, while data handling is with Berkeley, Oslo, Stockholm and Uppsala. The institute in Moscow contributes to the co-ordination with Russian spacecraft. The institutes in Ithaca, Greenbelt/GSFC, Boston (Phillips Lab.) and Minneapolis are mainly contributing to theoretical support and co-investigators at other institutes not mentioned above contribute to the co-ordination with the wave consortium of which EFW is a part.

References

1. Boehm, M.H., Carlson, C.W., McFadden, J. & Mozer, F.S., *Geophys Res. Lett.* **11**, 511 (1984).
2. Heelis, R.A., Foster, J.C., Beaujardiere, O. de la & Holt, J., *J. Geophys. Res.* **88**(10), 111 (1983).
3. Marklund, G.T., Heelis, R.A. & Winningham, J.D., *Can. J. Phys.* **64**, 1417 (1986).
4. Block, L.P., Fälthammar, C.-G., Lindqvist, P.-A., Marklund, G., Mozer, F.S. & Pedersen, A., *Geophys. Res. Lett.* **14**, 435 (1987).
5. Fälthammar, C.-G., Block, L.P., Lindqvist, P.-A., Marklund, G., Pedersen, A. & Mozer, F.S., *Annales Geophysicae* **5**(4) (1987).
6. Marklund, G.T., Blomberg, L.G., Potemra, T.A., Murphree, J.S., Rich, F.J. & Stasiewicz, K., *Geophys. Res. Lett.* **14**, 329 (1987).
7. Erickson, G.M. and Wolf, R.A., *Geophys. Res. Lett.* **7**, 900 (1980).
   Schindler, R. & Birn, J., *J. Geophys. Res.* **87**, 2263 (1982).
8. Dhont, J., Cattell, C.A. & Mozer, F.S., *EOS*, **67**, 1173 (1986).
9. Cattell, C.A., Mozer, F.S., Hones, Jr., E.W., Anderson, R.R. & Sharp, R.D., *J. Geophys. Res.* **91**, 5663 (1986).
10. Pedersen, A., Cattell, C.A., Fälthammar, C.-G., Formisano, V., Lindqvist, P.-A., Mozer, F.S. & Torbert, R.B., *Space Sci. Rev.* **37**, 269 (1984).
11. Cattell, C.A. and Mozer, F.S., *AGU Mon* **30**, 208 (1984).
12. Pedersen, A., Cattell, C.A., Fälthammar, C.-G., Knott, K., Lindqvist, P.-A., Manka, R.H. & Mozer, F.S., *J. Geophys. Res.* **90**, 1231 (1985).
13. Boström, R., Gustafsson, G., Holback, B., Holmgren, G., Koskinen, H. & Kintner, P., *Phys. Rev. Lett.* **61** (1988).